The Journal of the Korean Society of
Coastal and Ocean Engineers
Vol. 6. No. 4. pp. 459~471. December 1994

Quasi-3D Wave-Induced Circulation Model
準 3次元的 沿岸流 模型

Jung Lyul Lee*
李 正 烈*

Abstract : A numerical scheme solving the quasi-3D wave-induced circulation is presented. The governing equations have been solved implicitly using a fractional step method in conjunction with the approximate factorization techniques. The equation of each step was discretized by the finite volume scheme which yields more accurate and conservative approximations than the schemes based on finite differences. Examples of computed nearshore current patterns are presented to demonstrate the validity of the model for typical situations through comparison with laboratory experimental data (Gourlay, 1974).

要 旨 : 쇄파작용에 기인한 준 3차원적 연안류 순환 모델의 수치 기법을 제시한다. 지배 방정식은 근사 factorization 기법과 fractional step method를 사용하여 음해법으로 수치해석 되었고 분할된 식은 유한 체적법으로 차분된다. 계산된 3차원적 연안류 패턴의 한 예로서 Gourlay(1974)의 실험자료와 비교하여 간접적으로 모델의 타당성을 검증한다.

1. INTRODUCTION

The effort in nearshore circulation modelling can generally be broken down into two related areas, namely, the cross-shore circulation and the long shore current generation, both inside and outside the surf zone.

The vertical profile of cross-shore current pattern has been studied during the past ten years for the simple two-dimensional case on the plane beach. Since the postulation of the driving mechanism by Nielsen and Sorensen (1970), the analytical treatment was first appeared by Dally (1980). Svendsen (1984) proposed a theoretical undertow model using the first order approximation technique in describing the breaking waves, and Hansen and Svensen (1984) further considered the effect of the bottom boundary layer in the undertow. More recently, as the study progresses, several ideas have been added. Okayasu *et al.* (1988) estimated undertow profiles based on the assumed mean shear stress and eddy viscosity, and Yamashita and Tsuchiya (1990) developed the numerical model which consists of surface and inner layers.

Wave-induced longshore currents within the nearshore zone may be generated by a number of mechanisms including an oblique wave approaching the shoreline, a longshore variations in wave breaking height, or the combination of the above. The need for the development of an adequate theory for longshore currents has attracted a large number of contributors since the pioneer paper of Putnam and Arthur (1945). The theory for longshore currents by Longuet-Higgins (1970) was a rather elegant analysis based on the concept of radiation stress. His model and the concept behind it are widely accepted. Most of the later attempts were more or less modifications on the original model. The longshore current profile has been proposed by a number of investigators (de Vriend and Stive, 1987; Svendsen and Lorenz, 1989); most of them assumed the profile to be equivalent to the logarithmic velo-

*韓國海洋硏究所 海洋工學部 (Ocean Engineering Division, Korea Ocean Research and Development Institute, Ansan P.O. Box 29, Ansan 425-600, Korea)

city profile found in uniform steady streaming flows.

Numerical modelling of nearshore wave-induced currents has also advanced considerably since some of the earlier developments by Noda *et al.* (1974) and Ebersole and Dalrymple (1979). Both of these earlier models were driven by a wave refraction model but with no current feedback. More recently, Yoo and O'Connor (1986b) developed a wave-induced circulation model based upon what could be classified as a hyperbolic type wave equation; Yan (1987) and Winer (1988) developed their interaction models based upon parabolic approximation of the wave equation. The nearshore circulation, which was predicted by all models listed above, deals primarily with the vertically-averaged longshore current. Any nearshore hydrodynamic model has not been developed yet in the three dimensional formulation. Recently, however, de Vriend and Stive (1987) improved the nearshore circulation model by a quasi-three dimensional approach, which employed a combined depth-integrated current model and a vertical profile model. They introduced a primary and secondary profile for velocity variation over depth and assumed the primary velocity profile to be the same in the cross-shore and longshore direction. This quasi-three dimensional approach can be the first attempt towards a fully three-dimensional prediction of the nearshore current pattern. Later, Svensen and Lorenz (1989) assumed that the equations in the cross-shore and longshore directions could be decoupled and solved the cross-shore and longshore motion independently of long coast with straight bottom contours. Subsequently, the vertical structure of the flow field inside the surf zone was investigated only for simple case of two-dimensional profiles. Most of the proposed surf zone models whether theoritical or numerical were also restricted to two-dimensional.

The purpose of this study is to present a numerical model of gravity waves and current motions in the nearshore region extending into the surf zone where the effects of turbulence due to wave breaking become important. The model is able to reproduce the three-dimensional features of nearshore zone flow such as surface onshore flow, undertow, longshore current, etc. The model developed here allows for applications to more general three-dimensional topographies.

2. NEARSHORE HYDRODYNAMIC MODELS

In the present model, the wave model and circulation model can be combined or separated through the control of the main program. Therefore, the model is basically applicable to the problems of shallow water wave propagation and nearshore cirlulations driven by tides, wind and/or waves-induced radiation stresses.

This study describes the nearshore hydrodynamic model for wave and current field in the nearshore zone. The main model is the circulation model for computing mean water surface and mean currents. The wave model is a sub-model used to determine the radiation stress which is required in the circulation model as the forcing mechanism. The wave model takes offshore wave conditions as input offshore and propagates into nearshore zone while accounts for various nearshore processes including shoaling, refraction, diffraction, reflection, and surf-zone wave breaking. The basic wave model is developed for an irrotational flow field with steady mean currents. Various modifications are incorporated to accommodate for breaking and bottom friction effects. Figure 1 illustrates the main structure of the wave-induced nearshore circulation model.

The governing equations for the nearshore circulation model are divided into three major computational steps: 1) advection, 2) diffusion, and 3) propagation, according to the fractional step method. Each time step is composed of x-and y-directional computations by the alternating direction implicit method which speeds up the algorithm. The current field is affected by wave characteristics which result from the wave model. Here, a wave model(HM I) of the same type as presented by Madsen and Larsen (1987) is used.

The quasi-3D circulation model is governed by the continuity and momentum equations integrated over depth by parameterizing the vertical structure of the currents. The model described herein may be considered as an approximation to the full three-

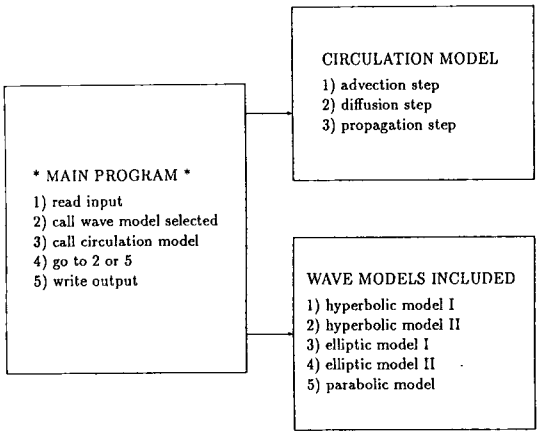

Fig. 1. Structural overview of nearshore hydrodynamic model.

dimensional model.

2.1 Depth-Integrated Circulation Model

The following mathemetical model is based on results obtained by Lee and Wang (1993a).
The continuity equation:

$$\frac{\partial \eta_c}{\partial t}+\frac{\partial}{\partial x}(Q_x+M_x)+\frac{\partial}{\partial y}(Q_y+M_y)=0 \tag{1}$$

The x-directional modified momentum equation:

$$\frac{\partial Q_x}{\partial t}+\frac{\partial}{\partial x}\left[\frac{Q_x^2}{h+\eta_c}+(h+\eta_c)T_{xx}\right]+\frac{\partial}{\partial y}\left[\frac{Q_xQ_y}{h+\eta_c}+(h+\eta_c)T_{xy}\right]+\frac{1}{\rho}\frac{\partial S_{xx}}{\partial x}+\frac{1}{\rho}\frac{\partial S_{yx}}{\partial y}+g(h+\eta_c)\frac{\partial \eta_c}{\partial x}-\frac{\tau_{Bx}}{\rho}+\frac{\tau_{Bx}}{\rho}=0 \tag{2}$$

The y-directional modified momentum equation:

$$\frac{\partial Q_y}{\partial t}+\frac{\partial}{\partial x}\left[\frac{Q_xQ_y}{h+\eta_c}+(h+\eta_c)T_{xy}\right]+\frac{\partial}{\partial y}\left[\frac{Q_y^2}{h+\eta_c}+(h+\eta_c)T_{yy}\right]+\frac{1}{\rho}\frac{\partial S_{xy}}{\partial x}+\frac{1}{\rho}\frac{\partial S_{yy}}{\partial y}+g(h+\eta_c)\frac{\partial \eta_c}{\partial y}-\frac{\tau_{By}}{\rho}+\frac{\tau_{By}}{\rho}=0 \tag{3}$$

where,

$$Q_x=\int_h^{\eta_c} u\,dz,\quad Q_y=\int_h^{\eta_c} v\,dz,$$

$$M_x=\frac{gH^2k_x}{8\sigma},\quad M_y=\frac{gH^2k_y}{8\sigma}$$

$$S_{xx}=E'\left[n(\cos^2\theta+1)-\frac{1}{2}+2\cos\theta\frac{u_s}{C}\right]$$

$$S_{xy}=S_{yx}=E'\left[\sin\theta\left(\cos\theta n+\frac{u_s}{C}\right)+\cos\theta\frac{v_s}{C}\right]$$

$$S_{yy}=E'\left[n(\sin^2\theta+1)-\frac{1}{2}+2\sin\theta\frac{v_s}{C}\right]$$

$$T_{xx}=\left[\frac{4C_{x1}^2}{45}+\frac{C_{x2}^2}{12}+\frac{C_{x1}C_{x2}}{6}\right]$$

$$T_{xy}=T_{yx}=\left[\frac{4C_{x1}C_{y1}}{45}+\frac{C_{x2}C_{y2}}{12}+\frac{C_{x1}C_{y2}}{12}+\frac{C_{x2}C_{y1}}{12}\right]$$

$$T_{yy}=\left[\frac{4C_{y1}^2}{45}+\frac{C_{y2}^2}{12}+\frac{C_{y1}C_{y2}}{6}\right]$$

where C_1, C_2 and C_3 of each axis are the coefficients of vertical current profile as given in the next section, and $E'=\rho gH^2/8$. The bottom friction consists of turbulent shear stress at the bottom, $\overline{\tau_{B,th}}$, and and bottom friction due to viscous and streaming flows, $\overline{\tau_{B,bf}}$

$$\tau_B=\overline{\tau_{B,th}}+\overline{\tau_{B,bf}}=F_w|u_{orb}|\bar{U}+F_c|u_{orb}|(U_B+U_{strm}) \tag{4}$$

where F_w is the wave friction factor varying over the wave breaking zone as given earier, while F_c is the current friction factor assumed constant here. The lateral shear stress is added to the momentum equations as

$$\tau_l=-\rho\left[\varepsilon_y\frac{\partial u}{\partial y}+\varepsilon_x\frac{\partial v}{\partial x}\right] \tag{5}$$

The mixing length coefficient, ε_x, is assumed to be proportional to the distance from the shoreline, $|x|$, multiplied by the shallow water phase speed as suggested by Longuet-Higgins (1970):

$$\varepsilon_x=N_x|x|\sqrt{g(h+\eta_c)}$$

It was suggested that a dimensionless constant N_x should be less than 0.016. The y-directional mixing length coefficient, ε_y, is assumed to be a constant everywhere.

2.2 Vertical Current Profile

A cross-shore circulation model is developed to

account for the effect of vertically nonuniform currents. Based upon theoretical solution of simple cases as well as laboratory measurements, the velocity profile may be approximated by a second order parabola (see Lee and Wang (1993a) for more details).

$$u=C_{x1}z'^2+C_{x2}z'+C_{x3} \tag{6}$$

$$v=C_{y1}z'^2+C_{y2}z'+C_{y3} \tag{7}$$

where z' is the nondimensional vertical axis, and C_1, C_2 and C_3 are determined in terms of discharge, Q, wave height, H, total depth, $h+\eta_c$, turbulent-induced bottom shear stress, $\tau_{B,th}$, and wind stress, τ_W as follows.

$$C_{x1}=-\frac{\eta_c+h}{2\varepsilon_z}\left\{\frac{g}{16}\frac{\partial H^2}{\partial x}-\frac{\overline{\tau_{Wx}}}{\rho}+\frac{\overline{\tau_{Bx,th}}}{\rho}\right\}$$

$$C_{x2}=-\frac{\eta_c+h}{\varepsilon_z}\left\{-\frac{g}{16}\frac{\partial H^2}{\partial x}+\frac{\overline{\tau_{Wx}}}{\rho}\right\}$$

$$C_{x3}=\frac{Q_x}{\eta_c+h}-\frac{C_{x1}}{3}-\frac{C_{x2}}{2}$$

$$C_{y1}=-\frac{\eta_c+h}{2\varepsilon_z}\left\{\frac{g}{16}\frac{\partial H^2}{\partial y}-\frac{\overline{\tau_{Wy}}}{\rho}+\frac{\overline{\tau_{By,th}}}{\rho}\right\}$$

$$C_{y2}=-\frac{\eta_c+h}{\varepsilon_z}\left\{-\frac{g}{16}\frac{\partial H^2}{\partial y}+\frac{\overline{\tau_{Wy}}}{\rho}\right\}$$

$$C_{y3}=\frac{Q_y}{\eta_c+h}-\frac{C_{y1}}{3}-\frac{C_{y2}}{2}$$

where,

$$\frac{\varepsilon_z}{\eta_c+h}=N_z|u_{orb}|,\quad \overline{\tau_{B,th}}=F_w|u_{orb}|\gamma U,$$

$$N_z=-\frac{\beta}{24(1-\gamma)\beta_L}\frac{\nabla\cdot(KH/k)}{(\beta-Cg/Cg_h)},$$

$$F_w=\frac{\beta}{4\gamma\beta_L}\frac{\nabla\cdot(KH/k)}{(\beta-Cg/Cg_h)},\ \text{and}\ |u_{orb}|=gH/2C.$$

2.3 Wave Prediction Model

The mild slope equation of elliptic type on wave-current interaction has been derived directly from the balance of mechanical energy on a wave-current coexisting field, which appeared to be the same as derived by Berkhoff (1972) although his expression was obtained for no current (Lee, 1994).

$$\nabla\cdot(CCg\nabla\hat{\phi})+(k^2CCg-i\mathbf{w}\sigma)\hat{\phi}=0 \tag{8}$$

where $\hat{\phi}$ is the velocity potential at mean water level, C is the relative phase velocity (σ/k), Cg is the relative group velocity ($\partial\sigma/\partial k$), k is the wave number determined by $\omega=\sigma+\bar{U}\cdot k$ as the absolute angular frequency, $\sigma=\sqrt{gk\tanh kh}$ as the relative angular frequency, $\mathbf{w}$ is the dissipation function, and $\nabla=i\partial/\partial x+j\partial/\partial y$, omitting the subscript h. In this section, the governing equations of the hyperbolic wave model are derived from the linearized MSE of elliptic type, Eq. (8) for waves interacting with currents. Equation (8) can be reduced to Helmohlz-type equation (Radder, 1979) without any essential loss of generality as

$$\nabla^2\phi+k_c^2\phi=0 \tag{9}$$

where $\phi=\sqrt{CCg}\hat{\phi}$, $k_c^2=k^2-\nabla^2(CCg)^{0.5}/(CCg)^{0.5}-i\mathbf{w}\sigma/CCg$. Equation (9) is particularly useful for the wave prediction in harhour since it encompasses shoaling, refraction, diffraction, and reflection effects of short waves, while it requires more than about ten grids per wave length.

Equation (9) can be written as a system of first order equations similar to the mass and momentum equations governing nearly horizontal flow in shallow water by use of the vector $\nabla\hat{\phi}$ and scalar ξ:

$$\frac{\partial\xi}{\partial t}+\frac{1}{k_c^2}\nabla\cdot(\nabla\phi)=0,\quad \frac{\partial\nabla\phi}{\partial t}+\nabla\xi=0 \tag{10}$$

where $\xi=\sqrt{CCg}\frac{g}{\sigma\omega}\eta$.

In order to speed up the solution considerably, the above equations are reformulated as done by Madsen and Larsen (1987):

$$\frac{\partial S}{\partial t}-i\omega S+\frac{1}{k_c^2}\nabla\cdot R=0,\quad \frac{\partial R}{\partial t}-i\omega R+\nabla S=0 \tag{11}$$

with $\xi=Se^{i\omega t}$ and $\nabla\hat{\phi}=Re^{i\omega t}$

Lee and Wang (1993b) has presented the analytical solutions of wave decay on a plane beach. However, their theoretical model can not be extended to the general bathymetry such as barred beachs. For an all-weather model, therefore, the wave decay model presented by Dally, *et al.* (1984) is used. They assumed that the dissipation rate is simply proportional to the difference between the local energy flux and that in the reformation zone, divided by

the local water depth. In terms of the dissipation function, w, the decay model can be written as

$$w=\frac{\Gamma_1 Cg}{h}\left(1-\frac{\Gamma_2^2 h^2}{H^2}\right) \tag{12}$$

where Γ_1 and Γ_2 are empirical constants. Dally, *et al.* (1984) suggested that $\Gamma_1=0.15$ and $\Gamma_2=0.4$ should be used. It is assumed that wave breaking occures when $H/h<0.4$.

3. ADI SCHEME

The main numerical technique follows that proposed by Rosenfeld *et al.* (1991) for solving time-dependent, three-dimensional incompressible Navier-Stokes equations in generalized coordinate systems. The governing equations obtained are solved by using a fractional step method in conjunction with the approximate factorization techniques leading to the implicit finite difference schemes. Since the time step of an explicit scheme is limited by the Courant-Friedrichs-Lewy (CFL) condition, it is advisable to reduce the number of time steps by use of an implicit scheme. It turns out that the implicit scheme accelerates the convergence of numerical calculations for the steady-state solutions. The finite-volume method can yield more accurate and conservative approximations than finite difference methods in generalized curvilinear coordinate systems and avoid problems with metric singularities that are usually associated with finite-difference methods since the flux integral form of equations is approximated in the finite volume of each grid cell as shown later. In addition, use of the finite volume method seems to allow the most effective implicit scheme even in the advection and diffusion steps. On a Cartesian grid system employed in the present model, the method reduces to a central-difference method inside the computational domain except for the boundary.

3.1 Fractional Step Method

A fractional step method is based on the recognition that the physical phenomena of water flow are represented by superimposing three individual operations such as advection, diffusion and propagation as Chorin (1968) pointed out. Therefore, momentum and continuity equations for the circulation model are divided into the following three elementary operations, while an equation set for the wave model forms a propagation operator itself:

◦ **Advection step:**

We solve the advective terms in conservation law form, including the radiation stress terms as:

$$\frac{\partial Q}{\partial t}+\frac{\partial \hat{F}}{\partial x}+\frac{\partial \hat{G}}{\partial y}=0 \tag{13}$$

◦ **Diffusion step:**

The effect of lateral mixing is added in this step.

$$\frac{\partial Q}{\partial t}+\frac{\partial \tilde{F}}{\partial x}+\frac{\partial \tilde{G}}{\partial y}=0 \tag{14}$$

◦ **Propagation step:**

$$\frac{\partial W}{\partial t}+A\frac{\partial W}{\partial x}+B\frac{\partial W}{\partial y}+Z=0 \tag{15}$$

For the circulation model, the propagation step is obtained by combining the remainder of the momentum equations with the continuity equation. The surface shear stress terms are omitted here:

$$W=(Q_x,\ Q_y,\ \eta_c)^T,\quad Z=\left(\frac{\overline{\tau_{Bx}}}{\rho},\ \frac{\overline{\tau_{By}}}{\rho},\ 0\right)^T,$$

$$A=\begin{pmatrix}0&0&gd\\0&0&0\\1&0&0\end{pmatrix},\qquad B=\begin{pmatrix}0&0&0\\0&0&gd\\0&1&0\end{pmatrix}$$

where d is the total water depth.

For the wave model:

$$W=(R_x,\ R_y,\ S)^T,\quad Z=(-i\omega R_x,\ -i\omega R_y,\ -i\omega S)^T$$

$$A=\begin{pmatrix}0&0&1\\0&0&0\\k_c^{\,2}&0&0\end{pmatrix},\qquad B=\begin{pmatrix}0&0&0\\0&0&1\\0&k_c^{\,2}&0\end{pmatrix}$$

3.2 Finite-Volume Discretization

Let N be the total amount of some property such as mass, momentum and energy within the system at time t. The equation of each step can be written in integral form

$$\frac{dN}{dt}=\frac{\partial}{\partial t}\int_\Omega Q\,d\Omega+\int_{\partial\Omega}F\,ds \tag{16}$$

where Ω is a fixed region with boundary $\partial\Omega$ and Q represents the conserved quantity and F is the corresponding flux term. Equation (16) is applied to each individual cell numbered by (i,j) to yield

$$\frac{dN}{dt} \cong \frac{\partial}{\partial t}(Q_{ij}\Delta\Omega_{ij}) + \sum_{k=1}^{N}(F_k \Delta S_k) \tag{17}$$

where N is the number of cell faces. The conserved variable Q_{ij} and the flow variable F_{ij} are taken at the center of each cell (i, j) as shown in Figure 2, hence the flow variable at each side F_k is taken as average of the two cell values on either side of that cell face, for example,

$$F_k = \frac{1}{2}(F_{i-1,j} + F_{ij})$$

Then, Eq. (17) can be expressed in terms of values at the center of grid cell as

$$\begin{aligned}\frac{dN}{dt} = &\frac{\partial}{\partial t}(Q_{ij}\Delta\Omega_{ij}) + \frac{1}{2}[(F_{i-1,j}+F_{ij})\Delta S_1 \\ &+(F_{i,j-1}+F_{ij})\Delta S_2 + (F_{i+1,j}+F_{ij})\Delta S_3 \\ &+(F_{i,j+1}+F_{ij})\Delta S_4]\end{aligned} \tag{18}$$

On a Cartesian grid system, let $|\Delta S_2|$ and $|\Delta S_4|$ reduce to Δx, and $|\Delta S_1|$ and $|\Delta S_3|$ to Δy, then $\Delta\Omega_{ij}$ reduces to $\Delta x\Delta y$. Consequently, this yields the central difference and is second-order accurate in space as

$$\begin{aligned}\frac{dN}{dt} = &\frac{\partial}{\partial t}(Q_{ij}\Delta x\Delta y) + \frac{1}{2}[-(F_{i-1,j}+F_{ij})\Delta y \\ &-(F_{i,j-1}+F_{ij})\Delta x + (F_{i+1,j}+F_{ij})\Delta y \\ &+(F_{i,j+1}+F_{ij})\Delta x]\end{aligned} \tag{19}$$

Let the time rate of N be zero, then the above equation becomes

$$\frac{\partial Q_{ij}}{\partial t} + \frac{1}{2}\left[\frac{F_{i+1,j}-F_{i-1,j}}{\Delta x} + \frac{F_{i,j+1}-F_{ij-1}}{\Delta y}\right] = 0 \tag{20}$$

The flux quantity should be given on the boundary as is usually done in the staggered grid system. Therefore, the flux quantity at the boundary is given, instead of averaging, as done in Eq. (8). Although the grid system employed here is the Cartesian, the reason why the finite volume method is applied is for 1) preparing for the curvilinear coordinate system, 2) locating the flux quantities at the grid center to lead the system of equations to tridigonal matrix form, and 3) preventing the metric singularities along the boundary.

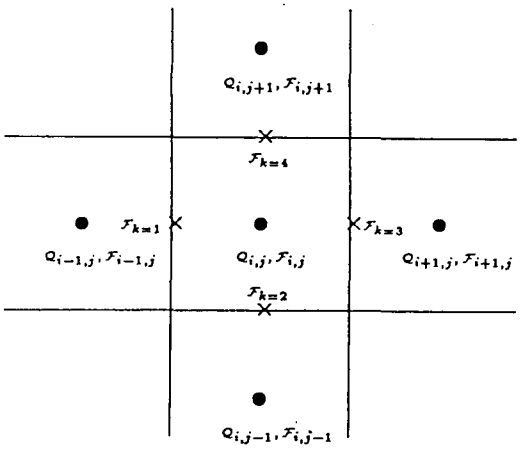

Fig. 2. Computational grid of finite volumetric scheme.

3.3 Approximate Factorizations

3.3.1 Implicit Formulation

Discretization of Eq. (13) yields

$$\begin{aligned}&\frac{Q_{ij}^{n+1/3} - Q_{ij}^{n}}{\Delta t} + \alpha(D_x\hat{F} + D_y\hat{G})_{ij}^{n+1/3} \\ &+(1-\alpha)(D_x\hat{F} + D_y\hat{G})_{ij}^{n} = 0\end{aligned} \tag{21}$$

where D_x and D_y are the standard central difference operators that approximate $\partial/\partial x$ and $\partial/\partial y$ and that are obtained through the finite volume discretization, and α is a parameter weighting the evaluation of spatial differences between the two time levels. Let the Jacobian matrices be

$$\hat{A} = \frac{\partial\hat{F}}{\partial Q} \quad \hat{B} = \frac{\partial\hat{G}}{\partial Q}$$

which can be approximated by assuming that wave characteristics are almost independent to velocity components to give

$$\hat{A} \approx \begin{Bmatrix} 2\frac{A_x}{d} & 0 \\ \frac{Q_y}{d} & \frac{Q_x}{d} \end{Bmatrix} \quad \hat{B} \approx \begin{Bmatrix} \frac{Q_y}{d} & \frac{Q_x}{d} \\ 0 & 2\frac{Q_y}{d} \end{Bmatrix}$$

and let the correction be

$$\Delta\hat{Q}^n = Q^{n+1/3} - Q^n$$

Linearization of the scheme may be achieved by approximating $\hat{F}^{n+1/3}$ and $\hat{G}^{n+1/3}$ by use of the Taylor series expansions about time level n,

$$\hat{F}^{n+1/3} \approx \hat{F}^n + \hat{A}\Delta\hat{Q},\quad \hat{G}^{n+1/3} \approx \hat{G}^n + \hat{B}\Delta\hat{Q}$$

Substituting into Eq. (21) gives

$$\Delta\hat{Q}_{ij}^n + \Delta t\alpha[D_x(\hat{A}\Delta\hat{Q})_{ij}^n + D_y(\hat{B}\Delta\hat{Q})_{ij}^n] = -\Delta t(D_x\hat{F} + D_y\hat{G})_{ij}^n \quad (22)$$

By factoring $\Delta\hat{Q}$,

$$[I + \Delta t\alpha(D_x\hat{A} + D_y\hat{B})_{ij}^n]\Delta\hat{Q}_{ij}^n = -\Delta t(D_x\hat{F} + D_y\hat{G})_{ij}^n \quad (23)$$

If α is zero, this form definitely reduces to the explicit type. A linear system of equations represented by Eq. (23) is too expensive and impractical for obtaining a solution. Therefore, an approximate factorization of the implicit operator is usually performed, as illustrated later.

Discretization of Eq. (14) yields

$$\frac{Q_{ij}^{n+2/3} - Q_{ij}^{n+1/3}}{\Delta t} + \alpha(D_x\tilde{F} + D_y\tilde{G})_{ij}^{n+2/3} + (1-\alpha)(D_x\tilde{F} + D_y\tilde{G})_{ij}^n = 0 \quad (24)$$

Let the Jacobian matrices be

$$\tilde{A} = \frac{\partial\tilde{F}}{\partial Q} \quad \tilde{B} = \frac{\partial\tilde{G}}{\partial Q}$$

which can be approximated by assuming that the total depth is almost independent of velocity components to give

$$\tilde{A} \approx \begin{Bmatrix} -2\varepsilon_x\dfrac{\partial}{\partial x}\left(\dfrac{1}{d}\right) & 0 \\ -\varepsilon_y\dfrac{\partial}{\partial y}\left(\dfrac{1}{d}\right) & -\varepsilon_x\dfrac{\partial}{\partial x}\left(\dfrac{1}{d}\right) \end{Bmatrix}$$

$$\tilde{A} \approx \begin{Bmatrix} -\varepsilon_y\dfrac{\partial}{\partial y}\left(\dfrac{1}{d}\right) & -\varepsilon_x\dfrac{\partial}{\partial x}\left(\dfrac{1}{d}\right) \\ 0 & -2\varepsilon_y\dfrac{\partial}{\partial y}\left(\dfrac{1}{d}\right) \end{Bmatrix}$$

and let the correction be

$$\Delta\tilde{Q}^n = Q^{n+2/3} - Q^n$$

Linearization of the scheme may be achieved by approximating $\hat{F}^{n+2/3}$ and $\hat{G}^{n+2/3}$ by use of the Taylor series expasions about time level n,

$$\tilde{F}^{n+2/3} \approx \tilde{F}^n + \tilde{A}\Delta\tilde{Q},\quad \tilde{G}^{n+2/3} \approx \tilde{G}^n + \tilde{B}\Delta\tilde{Q}$$

Substituting into Eq. (24) gives

$$\Delta\tilde{Q}_{ij}^n + \Delta t\alpha[D_x(\tilde{A}\Delta\tilde{Q})_{ij}^n + D_y(\tilde{B}\Delta\tilde{Q})_{ij}^n] = -\Delta t(D_x\tilde{F} + D_y\tilde{G})_{ij}^n + \Delta\hat{Q}^n \quad (25)$$

By factoring $\Delta\tilde{Q}$,

$$[I + \Delta t\alpha(D_x\tilde{A} + D_y\tilde{B})_{ij}^n]\Delta\tilde{Q}_{ij}^n = -\Delta t(D_x\tilde{F} + D_y\tilde{G})_{ij}^n + \Delta\hat{Q}^n \quad (26)$$

Discretization of Eq. (15) yields

$$\frac{W_{ij}^{n+1} - W_{ij}^{n+2/3}}{\Delta t} + \alpha(AD_xW + BD_yW)_{ij}^{n+1} + (1-\alpha)(AD_xW + BD_yW)_{ij}^n + Z_{ij} = 0 \quad (27)$$

Let the correction be $\Delta W^n = W^{n+1} - W^n$ by factoring ΔW,

$$[I + \Delta t\alpha(A_{ij}^n D_x + B_{ij}^n D_y)]\Delta W_{ij}^n = -\Delta t(AD_xW + BD_yW + Z)_{ij}^n + \Delta\tilde{W}^n \quad (28)$$

3.3.2 ADI Factorization

The scheme (23) is reduced to the alternating direction implicit (ADI) scheme by a product of two one-dimensional operators,

$$[I + \Delta t\alpha D_x\hat{A}_{ij}^n][I + \Delta t\alpha D_x\hat{B}_{ij}^n]\Delta\hat{Q}_{ij}^n = -\Delta t(D_x\hat{F} + D_y\hat{G})_{ij}^n \quad (29)$$

which can be inverted in two advanced time levels for one complete application to the two-dimensional system as

$$[I + \Delta t\alpha D_x\hat{A}_{ij}^n]\Delta\hat{Q}_{ij}^{*n} = -\Delta t(D_x\hat{F} + D_y\hat{G})_{ij}^n \quad (30)$$

$$[I + \Delta t\alpha D_y\hat{B}_{ij}^n]\Delta\hat{Q}_{ij}^n = \Delta\hat{Q}_{ij}^{*n} \quad (31)$$

Each unknown quantity in the left hand side is expressed implicitly at the advanced time level, and each right hand side is expressed explicitly in terms of known values. This scheme is unconditionally stable for the linear case if $\alpha \geq 1/2$. Expanding Eq. (30) into x and y components, respectively,

$$\Delta\hat{Q}_x^{*n} + 2\Delta t\alpha\left[D_x\left(\frac{\hat{Q}_x}{d}\Delta Q_x\right)\right]^{*n} = -\Delta t\left[gh\frac{\partial}{\partial x}\left(\frac{Q_x^2}{d} + \frac{S_{xx}}{\rho} + dT_{xx}\right)\right.$$

$$+D_y\left(\frac{Q_yQ_y}{d}+\frac{S_{yy}}{\rho}+dT_{yy}\right)\Big]^n \quad (32)$$

$$\Delta\hat{Q}_x^{*n}+\Delta t\alpha\Big[D_x\Big(\frac{Q_y}{d}\Delta\hat{Q}_x+\frac{Q_x}{d}\Delta\hat{Q}_y\Big)\Big]^{*n}=$$
$$-\Delta t\Big[D_x\Big(\frac{Q_xQ_y}{d}+\frac{S_{xy}}{\rho}+dT_{xy}\Big)$$
$$+D_y\Big(\frac{Q_y^2}{d}+\frac{S_{yy}}{\rho}+dT_{yy}\Big)\Big]^n \quad (33)$$

and expanding Eq. (31),

$$\Delta Q_x^n+\Delta t\alpha\Big[D_x\Big(\frac{Q_y}{d}\Delta Q_x+\frac{Q_x}{d}\Delta Q_y\Big)\Big]^n=\Delta Q_x^{*n} \quad (34)$$

$$\Delta Q_y^n+2\Delta t\alpha\Big[D_y\Big(\frac{Q_y}{d}\Delta Q_y\Big)\Big]^n=\Delta Q_y^{*n} \quad (35)$$

For the diffusion step, the scheme (26) is also reduced to the ADI scheme as

$$[I+\Delta t\alpha D_x\ \tilde{A}_{ij}^n]\Delta\tilde{Q}_{ij}^{*n}=-\Delta t(D_x\tilde{F}+D_y\tilde{G})_{ij}^n+\Delta\hat{Q}_{ij}^n \quad (36)$$

$$[I+\Delta t\alpha D_y\ \tilde{B}_{ij}^n]\Delta\tilde{Q}_{ij}^n=\Delta\tilde{Q}_{ij}^{*n} \quad (37)$$

Expanding Eqs. (36) and (37),

$$\Delta\tilde{Q}_x^{*n}-\Delta t\alpha\Big[D_x\Big(2\varepsilon_xD_x\frac{1\Delta\tilde{Q}_x}{d}\Big)\Big]^{*n}=$$
$$\Delta t\Big[D_x\Big(\varepsilon_xD_x\frac{Q_x}{d}\Big)+D_y\Big(\varepsilon_yD_y\frac{Q_x}{d}\Big)\Big]^n+\Delta\hat{Q}_x^n \quad (38)$$

$$\Delta\tilde{Q}_y^{*n}-\Delta t\alpha\Big[D_y\Big(\varepsilon_yD_y\frac{\Delta\tilde{Q}_x}{d}+\varepsilon_yD_x\frac{\Delta\tilde{Q}_y}{d}\Big)\Big]^{*n}=$$
$$\Delta t\Big[D_x\Big(\varepsilon_xD_x\frac{Q_x}{d}\Big)+D_y\Big(\varepsilon_yD_y\frac{Q_x}{d}\Big)\Big]^n+\Delta\ \hat{Q}_y^n \quad (39)$$

$$\Delta\tilde{Q}_x^n-\Delta t\alpha\Big[D_y\Big(2\varepsilon_yD_y\frac{\Delta\tilde{Q}_x}{d}+\varepsilon_yD_x\frac{\Delta\tilde{Q}_y}{d}\Big)\Big]^n=\Delta\tilde{Q}_x^{*n} \quad (40)$$

$$\Delta\ Q_y^n-\Delta t\alpha\Big[D_y\Big(2\varepsilon_yD_y\frac{\Delta\tilde{Q}_y}{d}\Big)\Big]^n=\Delta\tilde{Q}_y^{*n} \quad (41)$$

The alternating direction implicit (ADI) scheme is applied to propagation step as

$$[I+\Delta t\alpha A_{ij}^nD_x][I+\Delta t\alpha B_{ij}^nD_y]\Delta W_{ij}^n=$$
$$-\Delta t(AD_xW+BD_yW+Z)_{ij}^n+\Delta\ \tilde{W}_{ij}^{*n} \quad (42)$$

which can be inverted in two steps

$$[I+\Delta\alpha A_{ij}^nD_x]\Delta W_{ij}^{*n}=$$
$$-\Delta t(AD_xW+BD_yW+Z)_{ij}^n+\Delta\ \tilde{W}_{ij}^{*n} \quad (43)$$

$$[I+\Delta t\alpha B_{ij}^nD_x]\Delta W_{ij}^n=\Delta W_{ij}^{*n} \quad (44)$$

Expanding Eqs. (43) and (44) for the circulation model;

$$\Delta Q_x^n+\Delta t\alpha d^nD_x\Delta\eta_c^{*n}=-\Delta t\Big[gdD_x\eta_c+\frac{\overline{\tau_{Bx}}}{\rho}\Big]^n+\Delta\tilde{Q}_x^n \quad (45)$$

$$\Delta\eta_c^{*n}+\Delta t\alpha D_x\Delta Q_x^n=-\Delta t[D_xQ_x+D_yQ_y]^n \quad (46)$$

$$\Delta Q_y^n+\Delta t\alpha d^nD_y\Delta\eta_c^n=-\Delta t\Big[gdD_y\eta_c+\frac{\overline{\tau_{By}}}{\rho}\Big]^n+\Delta\ \tilde{Q}_y^n \quad (47)$$

$$\Delta\eta_c^n+\Delta t\alpha D_y\Delta Q_y^n=-\Delta\eta_c^{*n} \quad (48)$$

and for the wave model;

$$k_c^2(1-i\omega\alpha\Delta t)\Delta S^{*n}+\alpha\Delta tD_x\Delta R_x^n=$$
$$\Delta t(i\omega k_c^2S-D_xR_x-D_yR_y)^n \quad (49)$$

$$(1-i\omega\alpha\Delta t)\Delta R_x^n+\alpha\Delta tD_x\Delta S^{*n}=\Delta t(i\omega R_x-D_xS)^n \quad (50)$$

$$k_c^2(1-i\omega\alpha\Delta t)\Delta S^{*n}+\alpha\Delta tD_y\Delta R_y^n=\Delta S^{*n} \quad (51)$$

$$(1-i\omega\alpha\Delta t)\Delta R_y^n+\alpha\Delta tD_y\Delta S^{*n}=\Delta t(i\omega R_y-D_yS)^n \quad (52)$$

The above finite difference equations form the tridiagonal matrix for each axis.

3.4 Formation to Tridiagonal Matrix

The tridiagonal algorithm is the one direct method that is used widely in solving difference equations because of its great efficiency. In order to use this algorithm, the coefficients of the difference equations should form a tridiagonal matrix. The finite volume method allows each grid point to be posed at the center of the grid cell so as to give a system of equations that retains the computationally advantageous tridiagonal form for both advection and diffusion steps. For the propagation step of the circulation model, however, the point of current vector U (u_U, v_D) is posed at the grid side to allow the tridiagonal matrix the same as the traditional staggered grid system shown in Figure 3.

Discretizations of Eqs. (32-35) by finite volumes

yield

$$\Delta\hat{Q}_x^{*n}+2\alpha\frac{\Delta t}{2\Delta x}[-(u_L\Delta\hat{Q}_x)_{i-1,j}+((u_R-u_L)\Delta\hat{Q}_x)_{ij}+((u_L\Delta\hat{Q}_x)_{i+1,j}]^{*n}=D_1$$

$$\Delta\hat{Q}_y^{*n}+2\alpha\frac{\Delta t}{2\Delta x}[-(u_L\Delta\hat{Q}_y)_{i-1,j}+((u_R-u_L)\Delta\hat{Q}_y)_{ij}+((u_L\Delta\hat{Q}_y)_{i+1,j}]^{*n}=D_2-\alpha\Delta t\left[D_x\frac{Q_y}{d}\Delta\hat{Q}_x\right]^{*n}$$

$$\Delta Q_x^{n}+2\alpha\frac{\Delta t}{2\Delta x}[(-v_D\Delta\hat{Q}_x)_{ij-1}+((v_U-v_D)\Delta\hat{Q}_x)_{ij}+(v_D\Delta\hat{Q}_x)_{ij+1}]^{n}=\Delta Q_x^{*n}$$

$$\Delta Q_y^{n}+2\alpha\frac{\Delta t}{2\Delta x}[(-v_D\Delta\hat{Q}_y)_{ij-1}+((v_U-v_D)\Delta\hat{Q}_y)_{ij}+(v_D\Delta\hat{Q}_y)_{ij+1}]^{n}=\Delta Q_y^{*n}-\alpha\Delta t\left[D_y\frac{Q_y}{d}\Delta Q_y\right]^{n}$$

where

$$D_1=-\Delta t\left[D_x\left(\frac{Q_x^2}{d}+\frac{S_{xx}}{\rho}+dT_{xx}\right)+D_y\left(\frac{Q_xQ_y}{d}+\frac{S_{xy}}{\rho}+dT_{xy}\right)\right]^{n}$$

$$D_2=-\Delta t\left[D_x\left(\frac{Q_xQ_y}{d}+\frac{S_{xy}}{\rho}+dT_{xy}\right)+D_y\left(\frac{Q_y^2}{d}+\frac{S_{yy}}{\rho}+dT_{yy}\right)\right]^{n}$$

$$u_R|_{ij}=u_L|_{i+1,j},\quad u_R|_{ij}=u_L|_{i+1,j}$$

Discretizations of Eqs. (38-41) yield

$$\Delta\tilde{Q}_x^{*n}-2\alpha\frac{\Delta t}{\Delta x^2}\left[\left(\varepsilon_L\frac{\Delta\tilde{Q}_x}{d}\right)_{i-1,j}-\left((\varepsilon_R+\varepsilon_L)\frac{\Delta\tilde{Q}_x}{d}\right)_{ij}+\left(\varepsilon_L\frac{\Delta\tilde{Q}_x}{d}\right)_{i+1,j}\right]^{*n}=D_3$$

$$\Delta\tilde{Q}_y^{*n}-\alpha\frac{\Delta t}{\Delta x^2}\left[\left(\varepsilon_L\frac{\Delta\tilde{Q}_y}{d}\right)_{i-1,j}-\left((\varepsilon_R+\varepsilon_L)\frac{\Delta\tilde{Q}_y}{d}\right)_{ij}+\left(\varepsilon_L\frac{\Delta\tilde{Q}_y}{d}\right)_{i+1,j}\right]^{*n}=D_4+\alpha\Delta tD_x\left[\varepsilon_xD_x\frac{\Delta\tilde{Q}_x}{d}\right]^{*n}$$

$$\Delta\tilde{Q}_x^{n}-2\alpha\frac{\Delta t}{\Delta x^2}\left[\left(\varepsilon_D\frac{\Delta\tilde{Q}_x}{d}\right)_{ij-1}-\left((\varepsilon_U+\varepsilon_D)\frac{\Delta\tilde{Q}_x}{d}\right)_{ij}+\left(\varepsilon_D\frac{\Delta\tilde{Q}_x}{d}\right)_{ij+1}\right]^{n}=\Delta\tilde{Q}_x^{*n}$$

$$\Delta\tilde{Q}_y^{n}-\alpha\frac{\Delta t}{\Delta x^2}\left[\left(\varepsilon_D\frac{\Delta\tilde{Q}_y}{d}\right)_{ij-1}-\left((\varepsilon_U+\varepsilon_D)\frac{\Delta\tilde{Q}_y}{d}\right)_{ij}+\left(\varepsilon_D\frac{\Delta\tilde{Q}_y}{d}\right)_{ij+1}\right]^{n}=\Delta\tilde{Q}_y^{*n}+\alpha\Delta tD_y\left[\varepsilon_yD_y\frac{\Delta\tilde{Q}_y}{d}\right]^{n}$$

$$D_3=\Delta t\left[D_x\left(\varepsilon_xD_x\frac{Q_x}{d}\right)+D_y\left(\varepsilon_yD_y\frac{Q_y}{d}\right)\right]^{n}+\Delta\hat{Q}_x^{n}$$

$$D_4=\Delta t\left[D_x\left(\varepsilon_xD_x\frac{Q_x}{d}\right)+D_y\left(\varepsilon_yD_y\frac{Q_y}{d}\right)\right]^{n}+\Delta\hat{Q}_y^{n}$$

$$\varepsilon_L|_{ij}=\left(\frac{\varepsilon_x|_{ij}+\varepsilon_x|_{i-1,j}}{2}\right),\quad \varepsilon_D|_{ij}=\left(\frac{\varepsilon_y|_{ij}+\varepsilon_y|_{i-1,j}}{2}\right)$$

$$\varepsilon_R|_{ij}=\varepsilon_L|_{i+1,j},\qquad \varepsilon_U|_{ij}=\varepsilon_D|_{i+1,j}$$

Discretizations of Eqs. (45-48) yield

$$\Delta u_L^{n}+\alpha g\frac{\Delta t}{\Delta x}[\eta_{c\,ij}-\eta_{c\,i-1,j}]^{*n}=-\Delta t\left[gD_x\eta_c+\frac{\overline{\tau_{Bx}}}{\rho d}\right]^{n}+\Delta\tilde{u}_L^{n}$$

$$\left(\Delta\frac{\eta_c}{d}\right)^{*n}+\alpha\frac{\Delta t}{\Delta x}[(u_R-u_L)_{ij}]^{n}=-\Delta t[D_xu_L+D_yv_D]^{n}$$

$$\Delta u_D^{n}+\alpha g\frac{\Delta t}{\Delta y}[\eta_{c\,ij}-\eta_{c\,ij-1}]^{*n}=-\Delta t\left[gD_y\eta_c+\frac{\overline{\tau_{By}}}{\rho d}\right]^{n}+\Delta\tilde{v}_D^{n}$$

$$\left(\Delta\frac{\eta_c}{d}\right)^{n}+\alpha\frac{\Delta t}{\Delta y}[(u_U-u_D)_{ij}]^{n}=\left(\frac{\Delta\eta_c}{d}\right)^{*n}$$

where

$$\Delta\tilde{u}_L^{n}=\frac{1}{2}\left[\left(\frac{\tilde{Q}_x}{d}\right)_{ij}+\left(\frac{\tilde{Q}_x}{d}\right)_{i-1,j}\right]$$

$$\Delta\tilde{v}_D^{n}=\frac{1}{2}\left[\left(\frac{\tilde{Q}_y}{d}\right)_{ij}+\left(\frac{\tilde{Q}_y}{d}\right)_{ij-1}\right]$$

Discretizations for the wave model are similar to those for the circulation model shown above.

Now we can obtain the tridiagonal matrix form of the resulting difference equations; the matrix coefficients are given according to each step and each direction.

4. MODEL RESULTS

4.1 Model Verification for Wave-Current Interaction

Wave-current interaction is compared for colline[illegible] wav[illegible] id current in constant deep water de-

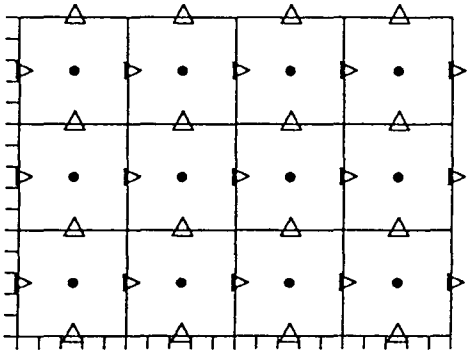

Fig. 3. Grid system of circulation model.

pth of 3 *m*. The given wave conditions are $H_i=0.1$ *m* at the upwave boundary and $T=1$ sec. Waves are allowed to pass freely through the downwave boundaries. The input data required for the model are given as follows; number of grids in x axis=101, number of grids in y axis=21, $\Delta x=0.1$ *m*, $\Delta y=0.1$ *m* and $\Delta t=1$ sec. The variation of resulting wave heights agree well with analytical solutions as shown in Figure 3. The implicit weighting parameter was given as 0.5.

The MSE of elliptic type given by Lee and Wang (1994) produces the finite wave height at the critical current speed which is regarded as the more reasonable result than the infinite wave height. If wave energy is fully propagated over a whole domain, we can assume that the stochastic characteristic of wave energy is governed by the MSE of elliptic type although the wave energy shows temporally unsteady state due to varying currents. Consequently, in this study, the MSE of elliptic type were used as the basic equation of numerical models predicting waves in semi-steady state.

5. COMPARISON WITH GOURLAY'S EXPERIMENTS

In order to examine the model capability more comprehensively, this section considers the complex situation in which all wave phenomena and interaction between waves and currents are involved.

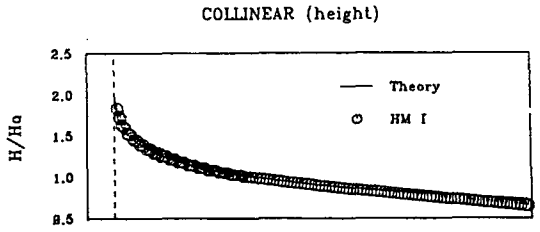

Fig. 4. Comparison with analytic solutions with results computed by HM I.

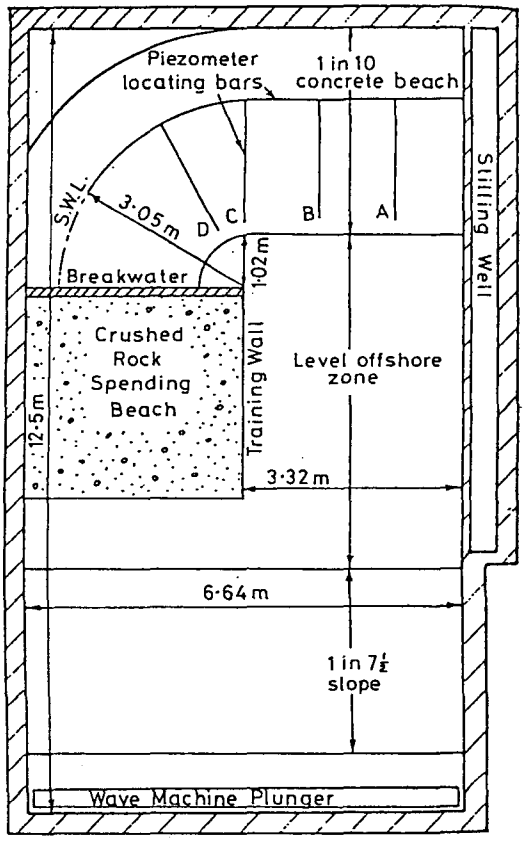

Fig. 5. Physical layout of Gourlay's experiment (1974).

Gourlay (1974) presented the circulation pattern generated in the lee of a shore-connected breakwater. Unfortunately, this experiment did not represent any three-dimensional patterns. Nevertheless, it corresponds with the request of this section at this moment. Figure 5 shows the physical layout of the experiment done by Gourlay for a water mass subjected to waves propagating normally at the open boundary. His experiment was perfomed for a wave

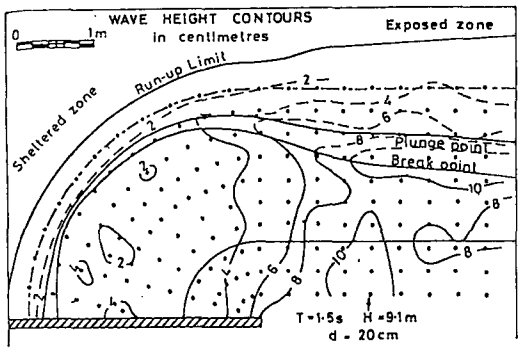

a)

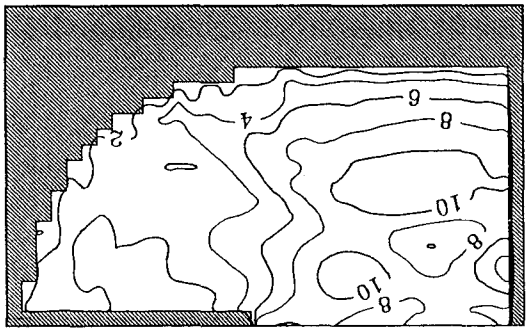

b)

Fig. 6. (a) Contour lines of measured heights (b) Computed height contours.

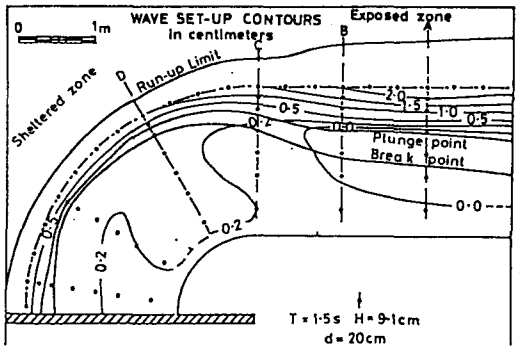

a)

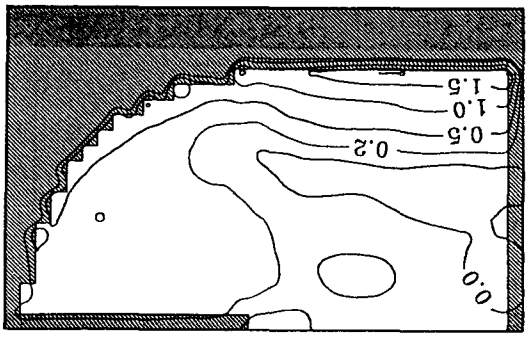

b)

Fig. 7. (a) Contours of measured set-ups (b) Computed set-up contours.

height of 9.1 centimeters with a wave period of 1.5 seconds. The contour lines of measured wave heights and set-ups are shown in Figures 6a and 7a, respectively. The current pattern is presented in Figure 8a. These experiments were compared with the model results obtained by Yoo and O'Connor (1986, 1988), Gaillard (1988), Winer (1988), and so on.

The wave model was coupled to provide the steady wave informations to the nearshore circulation model. For the numerical computation the grid size of 19.9 centimeters and the time step of 0.3 sec. were used. The steady state solutions could be obtained by 100 iterations. In the circulation model, six parameters are required; the implicit weighting parameter for the numerical scheme, α, was given as 1, the friction factor, $F_c = 0.02$, the shape factor, $\gamma = 0.98$, $\beta_f = 5.0$, and the horizontal mixing coefficients, ε_1 and ε_2 were given as 0.016 and 0.02, respectively. In the wave model, mainly two parameters are required; ratio of wave height to water depth at a breaking point, κ was given as 0.78, and the β which is employed in the wave breaking model was given as 1.15 for the slope of 1:10.

The results of wave height in the wave-current interaction field are compared in centimeter unit in Figure 6b, and those of set-up in Figure 7b. As shown in Fig. 8b, both circulations at the right upper corner and at the left lower corner appeared in the numerical results and the overall current pattern agreed reasonably with the measurement. From Figure 9a it becomes obvious that the quasi-three dimensional model can describe the surface velocity pattern measured by the particle moving with the residual wave fluctuation. Figure 9b shows the bottom velocity which is believed to affect the sediment transport.

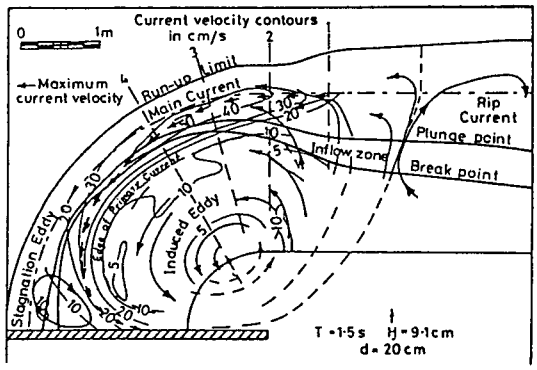

a)

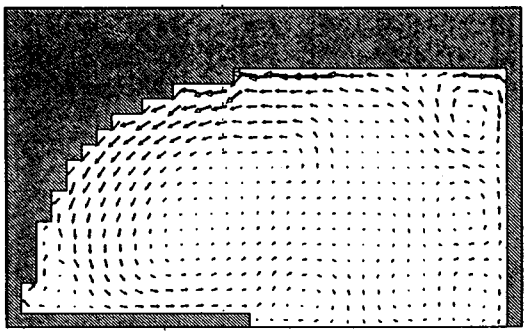

b)

Fig. 8. (a) Measured current pattern (b) Computed depth-averaged currents.

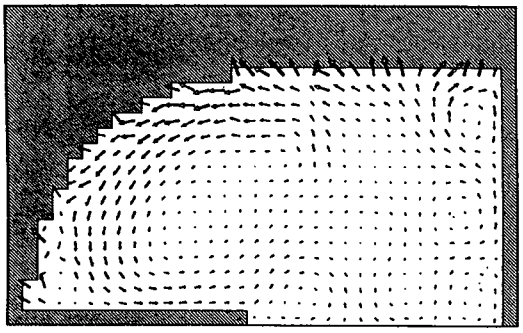

a)

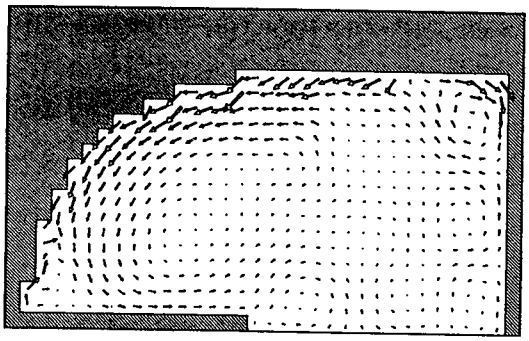

b)

Fig. 9. (a) Surface current pattern (b) Bottom current pattern.

6. CONCLUSIONS

The numerical method for solving the integrated quasi-three dimensional, unsteady, nearshore hydrodynamic model is presented utilizing the fractional step method in conjunction with the approximated ADI factorization techniques leading to an implicit scheme. The hydrodynamic model is composed of hyperbolic-type wave model and circulation model so that they could be effectively combined together. The employment of finite-volume discretization on a staggered mesh leads to a set of tridiagonal systems of equations that are easy to solve.

The mathematical quasi-3D model has already been compared with surf zone properties on uniform slope (Lee and Wang, 1993a). In this study, the numerical model is successfully applied to obtain the variations of wave height, onshore and longshore currents giving a reasonable agreement with labolatory experimental data (Gourlay, 1974).

REFERENCES

Berkhoff, J.C.W. 1972. Computation of combined refraction-diffraction, *Proc. 13th ICCE*, ASCE, pp. 471-490.

Bretherton, F.P., and Garrett, C.J.R. 1969. Wave trains in inhomogeneous moving media, *Proc. Royal Society of London*, London, England, A **302**: 529-554.

Dally, W.R. 1980. A numerical model for beach profile evolution, Master's Thesis, Civil Eng., Univ. of Delaware, Dept., Newark.

Dally, W.R., Dean, R.G., and Dalrymple, R.A. 1984. Modeling wave transformations in the surf zone, U.S. Army Engineer Waterways Experiment Station, Miscellaneous Paper CERC, 84-8.

de Vriend, H.J., and Stive, M.J.F. 1987. Quasi-3D modelling of nearshore currents, *Coastal Eng.*, **11**: 565-601.

Ebersole, B.A., Cialone, M.A. and Prater, M.D. 1986. Regional coastal processes numerical modeling system, Report 1, RCPWWAVE-A linear wave propagation model for engineering use, Technical report CERC-86-4, US Army Engineer WES, Vicksburg, Mississippi.

Ebersole, B.A., and Dalrymple, R.A. 1979. A numerical model for nearshore circulation including convective accelerations and lateral mixing, Ocean Engineering Report No. 21, Dept. of Civil Eng., Univ. of Delaware, Newark, Delaware.

Gaillard, P. 1988. Numerical modelling of wave-induced currents in the presence of coastal structures, *Coastal Eng.*, **12**: 63-81.

Gourlay, M.R. 1974. Wave set-up and wave generated currents in the lee of a breakwater or headland, *Proc. 14th ICCE*, ASCE, Copenhagen, 1976-1995.

Kirby, J.T. 1984. A note on linear surface wave-current interaction over slowly varying topography, *J. Geophys. Res.*, **89**(C1): 745-747.

Lee, J.L. 1993. Wave-current interaction and quasi-three dimensional modelling in nearshore zone, Ph.D dissertation, Coastal and Oceanographic Engineering Department, Univ. of Florida, Gainesville.

Lee, J.L. 1994. Mild slope equation of elliptic type in wave-current interaction, *J. the Korean Society of Coastal and Ocean Engineers*, **6**(1), pp. 51-60.

Lee, J.L. and Wang, H. 1992. Evaluation of numerical models on wave-current interactions, *Proc. 23rd ICCE*, ASCE, pp. 432-446.

Lee, J.L. and Wang, H. 1993a. Mathematical model for 3-dimensional circulation in surf zone, *J. the Korean Society of Coastal and Ocean Engineers*, **5**(4), pp. 369-383.

Lee, J.L. and Wang, H. 1993b. New approach for surf zone dynamics, *J. the Korean Society of Coastal and Ocean Engineers*, **5**(4), pp. 384-394.

Lee, J.L. and Wang, H. 1994. Wave modelling on wave-current interaction, *Proc. International Symposium: Waves-Physical and Numerical Modelling*, IAHR, pp. 941-950.

Longuet-Higgins, M.S. 1970. Longshore currents generated by obliquely incident sea waves, I, *J. Geophys. Res.*, **75**(33): 6778-6789.

Longuet-Higgins, M.S. and Stewart, R.W. 1961. The changes in amplitude of short gravity waves on steady non-uniform currents, *J. Fluid Mech.*, **10**: 529-549.

Madsen, P.A., and Larsen, J. 1987. An efficient finite-difference approach to the mild-slope equation, *Coastal Eng.*, **11**: 329-351.

Nielson, D.M., and Sorensen, T. 1970. Sand transport phenomena on coasts with bars, *Proc. 12th ICCE*, ASCE, pp. 855-866.

Noda, E., Sonu, C.J., Rupert, V.C., and Collins, J.I. 1974. Nearshore circulation under sea breeze conditions and wave-current interactions in the surf zone, Tetra Tech Report TC-149-4.

Okayasu, A., Shibayama, T., and Horikawa, K. 1988. Vertical variation of undertow in the surf zone, *Proc. 21st ICCE*, ASCE, pp. 478-491.

Putnam, J.A., and Arthur, R.S. 1948. Diffraction of water waves by breakwaters, *Trans. Am. Geophys. Union*, **29**: 481-490.

Radder A.C. 1979. On the parabolic equation for water-wave propagation, *J. Fluid Mech.*, **95**: 159-176.

Svendsen, I.A. 1984. Wave heights and set-up in a surf zone, *Coastal Eng.*, **8**: 303-329.

Svendsen, I.A., and Lorenz, R.S. 1989. Velocities in combined undertow and longshore currents, *Coastal Eng.*, **13**: 55-79.

Wang, H., Lin, L., Zhong, H., and Miao, G. 1991. Sebastian Inlet physical model studies. Part I-Fixed bed model, UFL/COEL-91/001, Coastal and Oceanographic Engineering Department, Univ. of Florida, Gainesville.

Winer, H.S. 1988. Numerical modeling of wave-induced currents using a parabolic wave equation, Ph.D dissertation, Coastal and Oceanographic Engineering Department, Univ. of Florida, Gainesville.

Yamashita, T., Tsuchiya, and Suriamihardja, D.A. 1990. Vertically 2-D nearshore circulation model, *Proc. 22nd ISCE*, ASCE, pp. 150-163.

Yan, Y. 1987. Numerical modeling of current and wave interaction on an inlet-beach system, Technical Report No. 73, Coastal and Oceanographic Engineering Department, Univ. of Florida, Gainesville.

Yoo, D., and O'Connor, B.A. 1986. Mathematical modeling of wave-induced nearshore circulations, *Proc. 20th ICCE*, ASCE, pp. 1667-1681.

Yoo, D., and O'Connor, B.A. 1988. Turbulence transport modelling of wave-induced currents, *Proc. Int. Cong. on Computer Modelling in Ocean Eng.* : 151-158.